Stability of the Human Respiratory Control System. Part II: Analysis of a three-dimensional delay state-space model

J. J. Batzel* H. T. Tran†

January 6, 1999

Abstract

A number of mathematical models of the human respiratory control system have been developed since 1940 to study a wide range of features of this complex system. Among them, periodic breathing (including Cheyne-Stokes respiration and apneustic breathing) is a collection of regular but involuntary breathing patterns that have important medical implications. The hypothesis that periodic breathing is the result of delay in the feedback signals to the respiratory control system has been studied since the work of Grodins et al. in the early 1950's [1]. The purpose of this paper is to study the stability characteristics of a feedback control system of five differential equations with delays in both the state and control variables presented by Khoo et al. [4] in 1991 for modeling human respiration. The paper is divided in two parts. Part I studies a simplified mathematical model of two nonlinear state equations modeling arterial partial pressures of O_2 and CO_2 and a peripheral controller. Analysis was done on this model to illuminate the effect of delay on the stability. It shows that delay dependent stability is affected by the controller gain, compartmental volumes and the manner in which changes in minute ventilation is produced (i.e., by deeper breathing or faster breathing). In adition, numerical simulations were performed to validate analytical results. Part II extends the model in Part I to include both peripheral and central controllers. This, however, necessitates the introduction of a third state equation modeling CO_2 levels in the brain. In addition to analytical studies on delay dependent stability, it shows that the decreased cardiac output (and hence increased delay) resulting from the congestive heart condition can induce instability at certain control gain levels. These analytical results were also confirmed by numerical simulations.

1 Introduction

The present Part II is a continuation of our companion paper "Stability of the Human Respiratory Control System. Part I: Analysis of a two-dimensional delay state-space

*Center for Research in Scientific Computation, Department of Mathematics, Box 8205, North Carolina State University, Raleigh, North Carolina, 27695-8205, (jjbatzel@unity.ncsu.edu).

†Center for Research in Scientific Computation, Department of Mathematics, Box 8205, North Carolina State University, Raleigh, North Carolina, 27695-8205, (tran@control.math.ncsu.edu).

model". The division in Parts I and II of this study is dictated by its overall length. In fact, Part II should be viewed as a continued study of Part I. In Part I, we have considered a two-dimensional model utilizing only the peripheral control. It was seen that this produces a system which is much more unstable than the five-dimensional model in the sense that the delay needed to introduce instability is only twice the normal delay of the system. Changes in control gain and cardiac output can push the system to unstable configurations. A modified control which included an approximation to the central control was also studied and it was found that the central control is integral to the stability of the system. However this control was physiologicaly inexact. It was clear that a compartment to monitor brain CO_2 levels which is the input to the central controller was needed to adequately model the respiratory control system. In Part II, we will look at the extension to the two-dimensional state space model which incorporates the compartment designed to model brain CO_2 levels.

2 A Three-Dimensional State Space Model

2.1 Model Equations

The following assumptions will be made:

(i) $P_{V_{CO_2}}$ = constant.

(ii) $P_{V_{O_2}}$ = constant.

(iii) $\dot{Q}$ = constant.

(iv) O_2 values stay within one section of the dissociation piecewise function.

(v) Only one delay is considered.

(vi) The delay to the brain compartment is the same as the peripheral delay.

(vii) The one delay is constant since $\dot{Q}$ is constant.

(viii) There is no modeling of breath by breath changes (constant flow model).

(ix) Dead space ventilation is represented by the ventilation factor E_F.

We note that these assumptions are the same as those used to derive the two-dimensional state space model in Part I. That is, the mathematical model is a nonlinear, autonomous system of three state equations modeling $P_{a_{CO_2}}$, $P_{a_{O_2}}$ and $P_{B_{CO_2}}$ with one constant delay. However, Part I only considered the peripheral controller which, consequently, eliminates the need for the equation for $P_{B_{CO_2}}$. In Part II, we consider both the central and peripheral controllers. Consequently, the state equations are:

$$\frac{dP_{a_{CO_2}}(t)}{dt} = \frac{863\dot{Q}K_{CO_2}[P_{V_{CO_2}}(t \Leftrightarrow \tau_V) \Leftrightarrow P_{a_{CO_2}}(t)] + E_F\dot{V}_I[P_{I_{CO_2}} \Leftrightarrow P_{a_{CO_2}}(t)]}{M_{L_{CO_2}}}, \quad (1)$$

$$\frac{dP_{a_{O_2}}(t)}{dt} = \frac{863\dot{Q}[m_v P_{v_{O_2}}(t-\tau_V) - m_a P_{a_{O_2}}(t) + B_v - B_a]}{M_{L_{O_2}}} + \frac{E_F \dot{V}_I [P_{I_{O_2}} - P_{a_{O_2}}(t)]}{M_{L_{O_2}}}, \tag{2}$$

$$\frac{dP_{B_{CO_2}}(t)}{dt} = \frac{MR_{B_{CO_2}}}{M_{B_{CO_2}} K_{B_{CO_2}}} + \frac{[\dot{Q}_B(P_{a_{CO_2}}(t-\tau_B) - P_{B_{CO_2}}(t))]}{M_{B_{CO_2}}}. \tag{3}$$

Recalling Section 2 of Part I and dropping the dot notation used by physiologists and refer to $\dot{V}_I$,$\dot{V}_C$, and $\dot{V}_P$ as V, V_C and V_P, the control equation is given by:

$$V = [[\ V_P\ ]] + [[\ V_C\ ]]$$

where

$$V_P = G_P \exp(-.05 P_{a_{O_2}}(t-\tau_a))(P_{a_{CO_2}}(t-\tau_a) - I_P)$$
$$V_C = G_C(P_{B_{CO_2}}(t) - \frac{MR_{B_{CO_2}}}{K_{CO_2}\dot{Q}_B} - I_C)$$

By the bracket notation, V_P and V_C are greater than or equal to zero. Note that V_P depends on $P_{a_{O_2}}$ and $P_{a_{CO_2}}$ while V_C depends on $P_{B_{CO_2}}$. Table 7 at the end of this paper gives parameter values used in simulation studies of the model (1)-(3) (unless otherwise noted).

2.2 Stability Analysis of the Three-Dimensional State Space Model

For the stability analysis of system (1), (2) and (3), we will rewrite it as:

$$\frac{dX(t)}{dt} = K_1[K_2 - X(t)] - K_3 V(X(t) - P_{I_{CO_2}}), \tag{4}$$
$$\frac{dY(t)}{dt} = K_4[K_5 - K_6 Y(t) - K_7] + K_8 V(K_9 - Y(t)), \tag{5}$$
$$\frac{dZ(t)}{dt} = K_9 + K_{10}(X(t-\tau) - Z(t)) \tag{6}$$

where

$$\begin{aligned} X(t) &= P_{a_{CO_2}}, \\ Y(t) &= P_{a_{O_2}}, \\ Z(t) &= P_{B_{CO_2}}, \\ V &= V(X(t-\tau), Y(t-\tau), Z(t)), \\ \tau &= \tau_a, \\ K_1 &= 863\frac{\dot{Q}K_{CO_2}}{M_{L_{CO_2}}}, \\ K_2 &= P_{V_{CO_2}}, \end{aligned}$$

$$
\begin{aligned}
\mathrm{K}_3 &= \frac{\mathrm{E_F}}{\mathrm{M_{L_{CO_2}}}}, \\
\mathrm{K}_4 &= 863\frac{\dot{\mathrm{Q}}}{\mathrm{M_{L_{O_2}}}}, \\
\mathrm{K}_5 &= \mathrm{m_v P_{V_{O_2}}} + \mathrm{B_v}, \\
\mathrm{K}_6 &= \mathrm{m_a}, \\
\mathrm{K}_7 &= \mathrm{B_a}, \\
\mathrm{K}_8 &= \frac{\mathrm{E_F}}{\mathrm{M_{L_{O_2}}}}, \\
\mathrm{K}_9 &= \frac{\mathrm{MR_{B_{CO_2}}}}{\mathrm{M_{B_{CO_2}} K_{B_{CO_2}}}}, \\
\mathrm{K}_{10} &= \frac{\dot{\mathrm{Q}}_\mathrm{B}}{\mathrm{M_{B_{CO_2}}}}.
\end{aligned}
$$

Note that V is increasing in both $X(\cdot)$ and $Z(\cdot)$ and decreasing in $Y(\cdot)$. Simplifying these equations gives

$$\frac{d\mathrm{X}(t)}{dt} = \mathrm{K}_{11} \Leftrightarrow \mathrm{K}_1\mathrm{X}(t) \Leftrightarrow \mathrm{K}_3\mathrm{V}(\mathrm{X}(t) \Leftrightarrow \mathrm{P_{I_{CO_2}}}), \tag{7}$$

$$\frac{d\mathrm{Y}(t)}{dt} = \mathrm{K}_{12} \Leftrightarrow \mathrm{K}_{13}\mathrm{Y}(t) + \mathrm{K}_8\mathrm{V}(\mathrm{P_{I_{O_2}}} \Leftrightarrow \mathrm{Y}(t)), \tag{8}$$

$$\frac{d\mathrm{Z}(t)}{dt} = \mathrm{K}_9 + \mathrm{K}_{10}(\mathrm{X}(t \Leftrightarrow \tau) \Leftrightarrow \mathrm{Z}(t)), \tag{9}$$

where

$$
\begin{aligned}
\mathrm{K}_{11} &= \mathrm{K}_1\mathrm{K}_2, \\
\mathrm{K}_{12} &= \mathrm{K}_4\mathrm{K}_5 \Leftrightarrow \mathrm{K}_7\mathrm{K}_4, \\
\mathrm{K}_{13} &= \mathrm{K}_4\mathrm{K}_6.
\end{aligned}
$$

Let

$$
\begin{aligned}
\mathrm{x}(t) &= \mathrm{X}(t) \Leftrightarrow \mathrm{P_{I_{CO_2}}}, \\
\mathrm{y}(t) &= \mathrm{P_{I_{O_2}}} \Leftrightarrow \mathrm{Y}(t), \\
\mathrm{z}(t) &= \mathrm{Z}(t),
\end{aligned}
$$

so that $\mathrm{x}(t)$ represents the difference in inspired CO_2 and arterial CO_2 and $\mathrm{y}(t)$ represents the difference in inspired O_2 and arterial O_2. We note that $\mathrm{P_{I_{CO_2}}} \approx 0$. We get upon substituting and simplifying:

$$\frac{d\mathrm{x}(t)}{dt} = \mathrm{a}_1 \Leftrightarrow \mathrm{a}_2\mathrm{x}(t) \Leftrightarrow \mathrm{a}_3\mathrm{V}\mathrm{x}(t), \tag{10}$$

$$\frac{d\mathrm{y}(t)}{dt} = \mathrm{b}_1 \Leftrightarrow \mathrm{b}_2\mathrm{y}(t) \Leftrightarrow \mathrm{b}_3\mathrm{V}\mathrm{y}(t), \tag{11}$$

$$\frac{d\mathrm{z}(t)}{dt} = \mathrm{c}_1 + \mathrm{c}_2\mathrm{x}(t \Leftrightarrow \tau) \Leftrightarrow \mathrm{c}_2\mathrm{z}(t), \tag{12}$$

where

$$\begin{aligned}
a_1 &= K_{11} \Leftrightarrow K_1 P_{I_{CO_2}}, \\
a_2 &= K_1, \\
a_3 &= K_3, \\
b_1 &= \Leftrightarrow K_{12} + K_{13} P_{I_{O_2}}, \\
b_2 &= K_{13}, \\
b_3 &= K_8, \\
c_1 &= \frac{MR_{B_{CO_2}}}{M_{B_{CO_2}} K_{CO_2}}, \\
c_2 &= \frac{\dot{Q}_B}{M_{B_{CO_2}}}.
\end{aligned}$$

In the control equation, V_C and V_P take the form

$$\begin{aligned}
V_C &= G_C(z(t) \Leftrightarrow \frac{c_1}{c_2} \Leftrightarrow I_C), \\
V_P &= G_P \exp \Leftrightarrow 0.05(P_{I_{O_2}} \Leftrightarrow y(t \Leftrightarrow \tau))(x(t \Leftrightarrow \tau) \Leftrightarrow I_P).
\end{aligned}$$

Again, we have dropped the brackets while always maintaining that V_P and V_C will be greater than or equal to zero. It should be noted that the control function V has the following properties:

(i) $V = V(x(t \Leftrightarrow \tau), y(t \Leftrightarrow \tau), z(t))$ and is now increasing in x, y and z;

(ii) $V_P = V_P(x, y)$, $V_C = V_C(z)$;

(iii) $V_P(I_P, y) = 0$, $V_C(\frac{c_1}{c_2} \Leftrightarrow I_C) = 0$;

(iv) V is differentiable for $x \neq I_P, z \neq \frac{c_1}{c_2} \Leftrightarrow I_C$;

(v) $V_X > 0$, $V_y > 0$, $V_Z > 0$ for $x > I_P$, $y > 0$ and $z > \frac{c_1}{c_2} \Leftrightarrow I_C$.

The above system (10), (11) and (12) is of the form

$$\dot{x}(t) = f(x_t).$$

where $f : C \to \mathbb{R}^3$ and $C = C([\Leftrightarrow r, 0], \mathbb{R}^3)$. $f(x_t)$ takes the form

$$f(x_t) = \begin{pmatrix} f_1(x_t) \\ f_2(x_t) \\ f_3(x_t) \end{pmatrix}$$

and $x(t)$ takes the form $(x_1(t), x_2(t), x_3(t))$. We now obtain existence and uniqueness of solutions to equations (10)-(12).

Theorem 2.1 *The system (10), (11) and (12) has a unique solution for* $\sigma \in \mathbb{R}$ *and* $\phi \in C$.

Proof. We will show that f is continuous on C and locally Lipschitz on compact sets of C. Recall that the norm on C is defined as follows. For $\phi \in C$,

$$|\phi|_\infty = \sup_{-r\le\theta\le 0} \sqrt{(\phi_1(\theta))^2 + (\phi_2(\theta))^2 + (\phi_3(\theta))^2},$$

It is clear that if each f_i is continuous and locally Lipschitz, for $i = 1, 2, 3$, then f is continuous and we can find a Lipschitz constant K for f.

Let $\vec{w} = (\vec{u}, \vec{v}) \in \mathbb{R}^3 \times \mathbb{R}^3$, where $\vec{u} = (u_1, u_2, u_3)$, $\vec{v} = (v_1, v_2, v_3)$ and with norm defined by $|(\vec{u}, \vec{v})|_{\mathbb{R}^3\times\mathbb{R}^3} = |\vec{u}|_{\mathbb{R}^3} + |\vec{v}|_{\mathbb{R}^3}$. Consider f_1 as a function defined on $\mathbb{R}^3 \times \mathbb{R}^3$ by

$$f_1(\vec{u}, \vec{v}) \;=\; \mathrm{a}_1 \Leftrightarrow \mathrm{a}_2 u_1 \Leftrightarrow \mathrm{a}_3 \mathrm{V}(v_1, v_2, u_3) u_1, \tag{13}$$

where

$$\begin{aligned} \mathrm{V}(v_1, v_2, u_3) \;=\; & \mathrm{G_P} \exp(\Leftrightarrow 0.05 v_2)(v_1 \Leftrightarrow \mathrm{I_P}) \\ & + \mathrm{G_C}(u_3 \Leftrightarrow \frac{\mathrm{c}_1}{\mathrm{c}_2} \Leftrightarrow \mathrm{I_C}). \end{aligned}$$

Since $\mathbb{R}^3\times\mathbb{R}^3 \cong \mathbb{R}^6$, it is clear that (13) is continuous on $\mathbb{R}^3\times\mathbb{R}^3$. From now on $|\cdot|$ will represent the appropriate norm when no confusion will occur. Let $\phi = (\phi_1, \phi_2, \phi_3) \in C$ be chosen and let $\vec{w} = (\vec{u}, \vec{v}) \in \mathbb{R}^3 \times \mathbb{R}^3$ where $(\vec{u}, \vec{v})$ is defined as:

$$\vec{u} = \begin{pmatrix} u_1 \\ u_2 \\ u_3 \end{pmatrix} = \begin{pmatrix} \phi_1(0) \\ \phi_2(0) \\ \phi_3(0) \end{pmatrix}, \vec{v} = \begin{pmatrix} v_1 \\ v_2 \\ v_3 \end{pmatrix} = \begin{pmatrix} \phi_1(\Leftrightarrow\tau) \\ \phi_2(\Leftrightarrow\tau) \\ \phi_3(\Leftrightarrow\tau) \end{pmatrix}.$$

Thus $\vec{w} = (\phi(0), \phi(\Leftrightarrow\tau))$ is a given element in $\mathbb{R}^3 \times \mathbb{R}^3$. Considering the right-hand side of (13) as a mapping on $\mathbb{R}^3 \times \mathbb{R}^3$, and for $\vec{w}$ defined above, for every $\epsilon = \epsilon(\vec{w}) > 0$ there is a $\delta > 0$ such that $|f_1(\vec{x}) \Leftrightarrow f_1(\vec{w})| < \epsilon$ when $|\vec{x} \Leftrightarrow \vec{w}| < \delta$. Let $|\phi \Leftrightarrow \psi| < \delta/2$ for $\psi \in C$. Then it follows that

$$|\phi(0) \Leftrightarrow \psi(0)| < \delta/2 \qquad \text{and} \qquad |\phi(\Leftrightarrow\tau) \Leftrightarrow \psi(\Leftrightarrow\tau)| < \delta/2.$$

For any ψ, let $\vec{x} = (\psi(0), \psi(\Leftrightarrow\tau))$. We have

$$|f_1(\psi) \Leftrightarrow f_1(\phi)| \;=\; |f_1(\vec{x}) \Leftrightarrow f_1(\vec{w})|$$

and

$$|f_1(\vec{x}) \Leftrightarrow f_1(\vec{w})| \;<\; \epsilon$$

when

$$\begin{aligned} |\vec{x} \Leftrightarrow \vec{w}| \;=\; & \sqrt{(\phi_1(0) \Leftrightarrow \psi_1(0))^2 + (\phi_2(0) \Leftrightarrow \psi_2(0))^2 + (\phi_3(0) \Leftrightarrow \psi_3(0))^2} \\ & + \sqrt{(\phi_1(\Leftrightarrow\tau) \Leftrightarrow \psi_1(\Leftrightarrow\tau))^2 + (\phi_2(\Leftrightarrow\tau) \Leftrightarrow \psi_2(\Leftrightarrow\tau))^2 + (\phi_3(\Leftrightarrow\tau) \Leftrightarrow \psi_3(\Leftrightarrow\tau))^2} \\ <\; & \delta. \end{aligned}$$

That is, when $|\phi \Leftrightarrow \psi| < \delta/2$. We conclude that f_1 is continuous on C. A similar argument can be given for f_2 and f_2 and thus f is continuous on C.

Again regarding f_1 as a mapping on $\mathbb{R}^3 \times \mathbb{R}^3$, it is clear that the exponential factor in $\mathrm{V_P}$ has continuous partial derivatives and will be locally Lipschitz on compact sets. Also, the second factor in $\mathrm{V_P}$ defined by the map $f : (\vec{u}, \vec{v}) \rightarrow [(v_1 \Leftrightarrow \mathrm{I_P})]$ is Lipschitz as is the mapping defining $\mathrm{V_C}$. Furthermore, sums and products of Lipschitz maps on compact sets will be Lipschitz. Therefore, the above mapping (13) will be locally Lipschitz on compact sets of $\mathbb{R}^3 \times \mathbb{R}^3$. Thus, if $\vec{x}, \vec{y} \in \mathbb{R}^3 \times \mathbb{R}^3$ are contained in a compact set, then there exists a $K > 0$ such that

$$|f_1(\vec{x}) \Leftrightarrow f_1(\vec{y})| \quad < \quad K|\vec{x} \Leftrightarrow \vec{y}| \tag{14}$$

Now, let D be a compact set in C. Hence, for $\phi = (\phi_1, \phi_2, \phi_3) \in D$, we have $|\phi| < b$ for some $b > 0$. Thus the set $\{\phi(t) | \phi \in D, t \in [\Leftrightarrow r, 0]\}$ will be contained in the closed ball $B(0, b)$, a compact set in $\mathbb{R}^3$ and so pairs of the form $(\phi(0), \phi(\Leftrightarrow \tau))$ will be contained in the closed ball $B(0, 2b)$ in $\mathbb{R}^3 \times \mathbb{R}^3$. This ball is compact and f_1 will be Lipschitz on $B(0, 2b)$ with Lipschitz constant K. Consider, for $\phi,\ \psi \in D$,

$$\begin{aligned} f_1(\phi) \Leftrightarrow f_1(\psi) \quad &= \quad \Leftrightarrow \mathrm{a}_2(\phi_1(0) \Leftrightarrow \psi_1(0)) \\ &\quad \Leftrightarrow \mathrm{a}_3(\mathrm{V}(\phi_1(\Leftrightarrow \tau), \phi_2(\Leftrightarrow \tau), \phi_3(0))\phi_1(0) \\ &\quad \Leftrightarrow \mathrm{V}(\psi_1(\Leftrightarrow \tau), \psi_2(\Leftrightarrow \tau), \psi_3(0))\psi_1(0)). \end{aligned}$$

Again considering the right-hand side of (13) as a mapping from $\mathbb{R}^3 \times \mathbb{R}^3$, and making the identification

$$\begin{pmatrix} u_1 \\ u_2 \\ u_3 \end{pmatrix} = \begin{pmatrix} \phi_1(0) \\ \phi_2(0) \\ \phi_3(0) \end{pmatrix}, \begin{pmatrix} v_1 \\ v_2 \\ v_3 \end{pmatrix} = \begin{pmatrix} \phi_1(\Leftrightarrow \tau) \\ \phi_2(\Leftrightarrow \tau) \\ \phi_3(\Leftrightarrow \tau) \end{pmatrix},$$

(similarly for ψ) we have

$$\begin{aligned} |f_1(\phi) \Leftrightarrow f_1(\psi)| \quad &< \quad K\sqrt{(\phi_1(0) \Leftrightarrow \psi_1(0))^2 + (\phi_2(0) \Leftrightarrow \psi_2(0))^2 + (\phi_3(0) \Leftrightarrow \psi_3(0))^2} \\ &\quad + K\sqrt{(\phi_1(\Leftrightarrow \tau) \Leftrightarrow \psi_1(\Leftrightarrow \tau))^2 + (\phi_2(\Leftrightarrow \tau) \Leftrightarrow \psi_2(\Leftrightarrow \tau))^2 + (\phi_3(\Leftrightarrow \tau) \Leftrightarrow \psi_3(\Leftrightarrow \tau))^2} \\ &\quad < 2K|\phi \Leftrightarrow \psi|. \end{aligned}$$

Thus f_1 is locally Lipschitz on compact sets. A similar argument can be given for f_2 and f_3 and thus f is locally Lipschitz. From well known results (see, e.g., [2] Theorems (2.2.1) and (2.2.3)) it follows that the system (10), (11) and (12) has a unique solution for $\sigma \in \mathbb{R}$ and $\phi \in C$. This ends the proof. □

Furthermore, from Theorem 2.2.2 in [2], we are also guaranteed that the solutions are continuously dependent on initial data so that the model is well-posed.

We now will show that the above system (10)-(12) has a unique positive equilibrium.

Theorem 2.2 *The above system described by (10),(11) and (12) has a unique positive equilibrium* $(\bar{x}^*, \bar{y}^*, \bar{z}^*)$.

Proof. At equilibrium, we have

$$\begin{aligned} 0 &= a_1 \Leftrightarrow a_2 x(t) \Leftrightarrow a_3 V x(t), && (15)\\ 0 &= b_1 \Leftrightarrow b_2 y(t) \Leftrightarrow b_3 V y(t), && (16)\\ 0 &= c_1 + c_2 x(t) \Leftrightarrow c_2 z(t). && (17) \end{aligned}$$

where $\bar{V} = V(\bar{x}, \bar{y})$. Note that $\frac{a_1}{a_2} = P_{V_{CO_2}}$ and will always be physiologically much larger than I_P, the threshold level for zero ventilation. This implies that $\bar{V} = 0$ is impossible at equilibrium. For then, $\bar{V} = 0 \Rightarrow \bar{x} \leq I_P$ but $\bar{V} = 0 \Rightarrow \bar{x} = \frac{a_1}{a_2}$ from solving (15) for $\bar{x}$ and this contradicts that $\frac{a_1}{a_2} >> I_P$. We get from the above at equilibrium relationships:

$$\bar{x} = \frac{a_1}{a_2 + a_3 \bar{V}}, \tag{18}$$

$$\bar{z} = \bar{x} + \frac{c_1}{c_2}, \tag{19}$$

$$\bar{V} = \frac{b_1}{b_3 \bar{y}} \Leftrightarrow \frac{b_2}{b_3}. \tag{20}$$

Note that this equation gives the value for $\bar{V}$ at equilibrium and is not meant as a formula for $\bar{V}$ in terms of $\bar{y}$. Substituting (20) into (18) gives

$$\bar{x} = \frac{a_1}{a_2 + a_3(\frac{b_1}{b_3 \bar{y}} \Leftrightarrow \frac{b_2}{b_3})}. \tag{21}$$

At equilibrium, $\bar{y} \geq \frac{b_1}{b_2} \Leftrightarrow \bar{V} \leq 0$. This is impossible at equilibrium so that $\bar{y} < \frac{b_1}{b_2}$. Now using (21),we see that $\bar{x} = x(\bar{y})$ is monotonically increasing in $\bar{y}$ and $\bar{x} \to 0$ monotonically as $\bar{y} \to 0$. Thus we may find a unique $\bar{y}$ such that $\bar{x}$ is as close to (but greater than) $\bar{x} = I_P$ as we wish. Furthermore, from the equation for V_P we may bound the exponential factor involving y on the interval $0 < y < \frac{b_1}{b_2}$ by a positive value M. Thus

$$V_P \leq M(x \Leftrightarrow I_P).$$

We can choose $\bar{x}$ so that V_P is as small as we wish and find a corresponding $\bar{y}$ using (21). Furthermore, in the expression for V_C if we set $K_{TC} = \frac{c_1}{c_2}$ then

$$\begin{aligned} V &= 0 \Rightarrow V_C = V_P = 0\\ &\Rightarrow \bar{x} \leq I_P \text{and } \bar{z} \leq I_C + K_{TC}. \end{aligned}$$

Since the parameters I_P and I_C are chosen (see [3]) so that $I_P = I_C$, from (19) we see that $\bar{x} \leq I_P \Rightarrow \bar{z} \leq I_C + K_{TC} \Rightarrow V = 0$.

We also note that

$$g(y) = \frac{b_1}{b_3 y} \Leftrightarrow \frac{b_2}{b_3}$$

is decreasing in y. By choosing $\bar{x}$ sufficiently close to $x = I_P$ (call it $\bar{x}_{I_P}$) we may find a triple $(\bar{x}_{I_P}, \bar{y}_{I_P}, \bar{z}_{I_P})$ such that $\bar{V}(\bar{x}_{I_P}, \bar{y}_{I_P}, \bar{z}_{I_P})$ is as small as we like and set up the relation

$$\bar{V}(\bar{x}_{I_P}, \bar{y}_{I_P}, \bar{z}_{I_P}) < g(\bar{y}_{I_P}). \tag{22}$$

where $\bar{y}_{I_P} < \frac{b_1}{b_2}$ (but close to $\frac{b_1}{b_2}$).

From (18), (19) and (20) we see that $\bar{x}$ is monotonically increasing in $\bar{y}$ and $\bar{z}$ is monotonically increasing in $\bar{x}$ and hence $\bar{y}$. $\bar{V}$ is increasing in $\bar{x}$, $\bar{y}$ and $\bar{z}$ so that we may consider $\bar{V}$ as an increasing function in $\bar{y}$, where $\bar{y}_{I_P} < \frac{b_1}{b_2}$. Also $g(y) = \frac{b_1}{b_3 y} \Leftrightarrow \frac{b_2}{b_3}$ is decreasing in y and $g(\frac{b_1}{b_2}) = 0$. Thus if we begin with the relation (22) there will be a unique solution $\bar{y}^*$ of

$$\bar{V}(\bar{x}(\bar{y}), \bar{y}) = \frac{b_1}{b_3 \bar{y}} \Leftrightarrow \frac{b_2}{b_3}$$

where $\bar{y}_{I_P} < \bar{y}^* < \frac{b_1}{b_2}$. Using the solution $\bar{y}^*$ to define $\bar{x}^*$ we get upon substituting $\bar{y}^*$ into (21) the corresponding uniquely defined $\bar{x}^*$:

$$\bar{x}^* = \frac{a_1}{a_2 + a_3(\frac{b_1}{b_3 \bar{y}^*} \Leftrightarrow \frac{b_2}{b_3})}.$$

Note that $I_P < \bar{x}^* < \frac{a_1}{a_2}$. Using $\bar{x}^*$ and (19) we find $\bar{z}^*$. Solving for $\bar{V}$ in (18) at equilibrium we see that

$$\bar{V} = \frac{a_1}{a_3 \bar{x}} \Leftrightarrow \frac{a_2}{a_3} \tag{23}$$

and substituting $\bar{x}^*$ defined above we get

$$\bar{V}(\bar{x}^*(\bar{y}^*), \bar{y}^*, \bar{z}^*(\bar{y}^*)) = \frac{a_1}{a_3 \left(\frac{a_1}{a_2 + a_3(\frac{b_1}{b_3}\bar{y}^* - \frac{b_2}{b_3})} \right)} \Leftrightarrow \frac{a_2}{a_3} = \frac{b_1}{b_3 \bar{y}^*} \Leftrightarrow \frac{b_2}{b_3}.$$

Thus $\bar{V}$ as defined by (20) and (18) are equal at $(\bar{x}^*, \bar{y}^*, \bar{z}^*)$ where $\bar{z}^*$ is defined by $\bar{x}^*$. We may conclude that there is a positive equilibrium $(\bar{x}^*, \bar{y}^*, \bar{z}^*)$ to the above system and it is unique. In addition, we have $\bar{x}^* > I_P$ and $\bar{z}^* > I_C + K_{TC}$. This completes our proof. □

We will now consider the stability of the above nonlinear system of delay differential equations. To this end, we first linearize equations (10),(11) and (12) about the

equilibrium solutions. Let:

$$\begin{aligned}\xi(t) &= \mathrm{x}(t) \Leftrightarrow \bar{\mathrm{x}},\\ \eta(t) &= \mathrm{y}(t) \Leftrightarrow \bar{\mathrm{y}},\\ \nu(t) &= \mathrm{z}(t) \Leftrightarrow \bar{\mathrm{z}}.\end{aligned}$$

We get

$$\begin{aligned}\frac{d\xi(t)}{dt} &= (\Leftrightarrow \mathrm{a}_2 \Leftrightarrow \mathrm{a}_3\bar{\mathrm{V}})\xi(t) \Leftrightarrow \mathrm{a}_3\bar{\mathrm{x}}\bar{\mathrm{V}}_{\mathrm{X}}\xi(t \Leftrightarrow \tau) \Leftrightarrow \mathrm{a}_3\bar{\mathrm{x}}\bar{\mathrm{V}}_{\mathrm{Y}}\eta(t \Leftrightarrow \tau) \Leftrightarrow \mathrm{a}_3\bar{\mathrm{x}}\bar{\mathrm{V}}_{\mathrm{Z}}\nu(t),\\ \frac{d\eta(t)}{dt} &= (\Leftrightarrow \mathrm{b}_2 \Leftrightarrow \mathrm{b}_3\bar{\mathrm{V}})\eta(t) \Leftrightarrow \mathrm{b}_3\bar{\mathrm{y}}\bar{\mathrm{V}}_{\mathrm{X}}\xi(t \Leftrightarrow \tau) \Leftrightarrow \mathrm{b}_3\bar{\mathrm{y}}\bar{\mathrm{V}}_{\mathrm{Y}}\eta(t \Leftrightarrow \tau) \Leftrightarrow \mathrm{b}_3\bar{\mathrm{y}}\bar{\mathrm{V}}_{\mathrm{Z}}\nu(t),\\ \frac{d\nu(t)}{dt} &= +\mathrm{c}_2\xi(t \Leftrightarrow \tau) \Leftrightarrow \mathrm{c}_2\nu(t).\end{aligned}$$

Again writing in matrix form we get

$$\frac{d}{dt}\begin{pmatrix}\xi(t)\\ \eta(t)\\ \nu(t)\end{pmatrix} = A\begin{pmatrix}\xi(t)\\ \eta(t)\\ \nu(t)\end{pmatrix} + B\begin{pmatrix}\xi(t \Leftrightarrow \tau)\\ \eta(t \Leftrightarrow \tau)\\ \nu(t \Leftrightarrow \tau)\end{pmatrix}.$$

Matrix A takes the form

$$A = \begin{pmatrix}\Leftrightarrow \mathrm{a}_2 \Leftrightarrow \mathrm{a}_3\bar{\mathrm{V}} & 0 & \Leftrightarrow \mathrm{a}_3\bar{\mathrm{x}}\bar{\mathrm{V}}_{\mathrm{Z}}\\ 0 & \Leftrightarrow \mathrm{b}_2 \Leftrightarrow \mathrm{b}_3\bar{\mathrm{V}} & \Leftrightarrow \mathrm{b}_3\bar{\mathrm{y}}\bar{\mathrm{V}}_{\mathrm{Z}}\\ 0 & 0 & \Leftrightarrow \mathrm{c}_2\end{pmatrix}$$

and matrix B has the form

$$B = \begin{pmatrix}\Leftrightarrow \mathrm{a}_3\bar{\mathrm{x}}\bar{\mathrm{V}}_{\mathrm{X}} & \Leftrightarrow \mathrm{a}_3\bar{\mathrm{x}}\bar{\mathrm{V}}_{\mathrm{Y}} & 0\\ \Leftrightarrow \mathrm{b}_3\bar{\mathrm{y}}\bar{\mathrm{V}}_{\mathrm{X}} & \Leftrightarrow \mathrm{b}_3\bar{\mathrm{y}}\bar{\mathrm{V}}_{\mathrm{Y}} & 0\\ \mathrm{c}_2 & 0 & 0\end{pmatrix}.$$

The characteristic equation is

$$\Delta(\lambda, \tau) = \mathrm{P}(\lambda) + \mathrm{Q}(\lambda)e^{-\tau\lambda} = 0 \tag{24}$$

where

$$\begin{aligned}\mathrm{P}(\lambda) &= \lambda^3 + (\mathrm{A}_1 + \mathrm{B}_1 + \mathrm{C}_1)\lambda^2 + (\mathrm{A}_1\mathrm{C}_1 + \mathrm{A}_1\mathrm{B}_1 + \mathrm{B}_1\mathrm{C}_1 + \mathrm{A}_1\mathrm{C}_1)\lambda + \mathrm{A}_1\mathrm{B}_1\mathrm{C}_1\\ \mathrm{Q}(\lambda) &= (\mathrm{A}_2 + \mathrm{B}_2)\lambda^2 + (\mathrm{B}_2\mathrm{C}_1 + \mathrm{A}_1\mathrm{B}_2 + \mathrm{A}_2\mathrm{C}_1 + \mathrm{A}_2\mathrm{B}_1 + \mathrm{C}_2\mathrm{C}_1)\lambda\\ &\quad +\mathrm{A}_1\mathrm{B}_2\mathrm{C}_1 + \mathrm{A}_2\mathrm{B}_1\mathrm{C}_1 + \mathrm{C}_2\mathrm{C}_1\mathrm{B}_1,\end{aligned}$$

and where

$$\begin{aligned} A_1 &= a_2 + a_3\bar{V}, \\ A_2 &= a_3\bar{x}\bar{V}_X, \\ B_1 &= b_2 + b_3\bar{V}, \\ B_2 &= b_3\bar{y}\bar{V}_Y, \\ C_1 &= c_2, \\ C_2 &= a_3\bar{x}\bar{V}_Z. \end{aligned}$$

Clearly $|P(i\omega)|^2 \Leftrightarrow |Q(i\omega)|^2$ will take a complicated form from which it is difficult to extract a simple condition for stability. However, we can study the stability for parameter values which are physiological meaningful (Table 7). The expression

$$F(\omega) = |P(i\omega)|^2 \Leftrightarrow |Q(i\omega)|^2$$

is a six degree polynomial of the form

$$F(\omega) = \omega^6 + k_1\omega^4 + k_2\omega^2 + k_3.$$

Now, we let $\omega^2 = v$ and define

$$\hat{F}(v) = v^3 + k_1 v^2 + k_2 v + k_3.$$

We find, for our parameters, that this cubic has two negative roots and one positive root v_o so that $\omega_o = \sqrt{v_o}$ is the only (simple) positive root of $F(\omega)$ (see Figure 1). Also we see that for these parameters :

- $\Delta(0, \tau) \neq 0$;
- $\Delta(\lambda, 0) = 0$ is a cubic with 3 negative roots (see Figure 2).

Extensive numerical tests varying control gain, cardiac output and threshold levels indicate that the graphs in Figures 1 and 2 shift somewhat as changes in the above mentioned parameters are made but the number and the nature of the roots do not change. In all of the simulations to be discussed below we have that:

- there are three negative roots of $\Delta(\lambda, 0)$;
- there is exactly one positive root for $F(\omega)$.

For the range between the most destabilizing combination of $\dot{Q}$, controller gain and lung compartment volumes and the most stabilizing combination, the two conditions listed above are satisfied. These conditions, together with the fact that P and Q are polynomials with real coefficients guarantees that the conditions required by Theorem 3.5 in Part I are satisfied.

Hence we may apply Theorem 3.5 described in Part I to look for τ which will produce instability. Once again there will be one cross over from stable to unstable behavior.

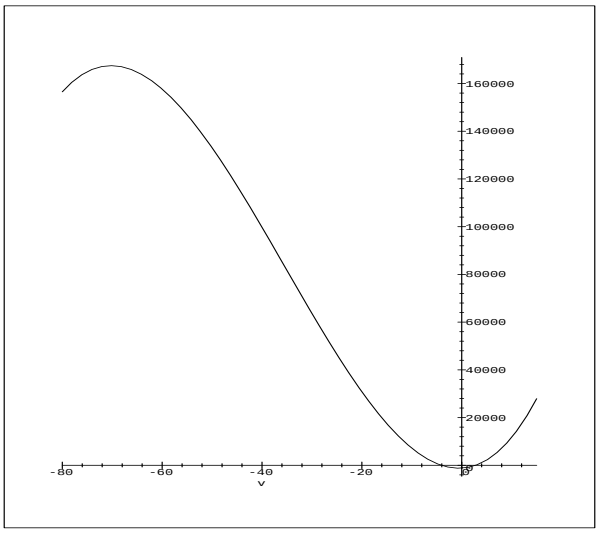

Figure 1: Roots of $\hat{F}(v)$ for the three-dimensional system

Figure 3 shows the stable solutions for the system (10), (11) and (12) and Figure 4 exhibits the unstable ones. In Figures 3 and 4, we also include the constant values for $P_{V_{CO_2}}$ and $P_{V_{O_2}}$. Table 1 gives the parameter values and stability calculations for the numerical solutions shown in Figures 3 and 4.

We can compare the results of the stability analysis for the two-dimensional model studied in Part I and the three-dimensional model presented here. We compare the two-dimensional model with the peripheral control only. Using the same parameter values (from the three-dimensional model parameters, Table 7) we see from Table 2 that a model with the peripheral control only is much more unstable than the three-dimensional model incorporating both a peripheral control and central control. Note that for normal control gain the two-dimensional model predicted instability at a τ multiplier of 1.94 while the three-dimensional model gives 11.26. We can also test these predictions against the five-dimensional model. Using the five-dimensional model (without breath by breath variation), numerical simulations indicated that instability occurs when the τ multiplier was 14.1 (see Table 2).

We see that the overall structure of instability was illuminated by the three-dimensional model and the actual state variables were in good agreement with the five-dimensional model. The τ multiplier necessary for instability for the five-dimensional model was about 28% higher than predicted by the smaller models indicating that the tissue compartments add to the stability of the system. Figure 5 represents the five-dimensional model simulation at instability. Note that $P_{V_{CO_2}}$ and $P_{V_{O_2}}$ do not vary much even in unstable situations.

Finally, we will present calculations comparing the effects produced by varying different parameters. We will introduce one further parameter in this analysis. We have heretofore used E_F set at 0.7 to reflect dead space ventilation V_D. This factor reduces

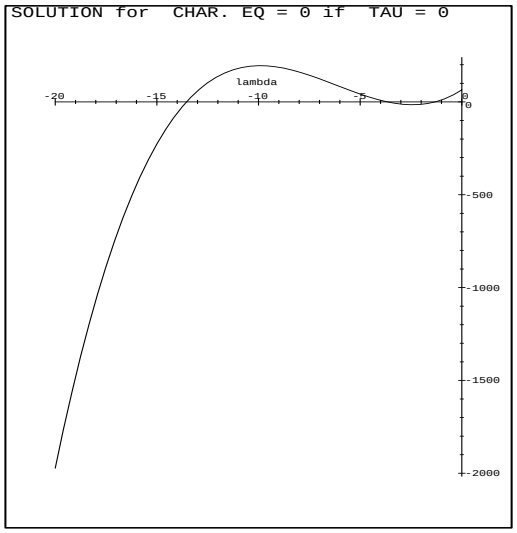

Figure 2: Roots of characteristic equation with $\tau = 0$ for the three-dimensional system

each breath by a certain percentage. In this case, we are assuming that an increase in minute ventilation is produced by increased breathing rate and thus each breath is reduced by the same dead space volume percentage. We might also assume that breathing rate is held constant and depth of breathing is varied. In this case there will be a fixed dead space volume subtracted from each breath as discussed in Section 2 of Part I. We then have $V_{\text{eff}} = V \Leftrightarrow V_D$. E_F will be set at 1.0. Notice that in this case V_D serves to reduce V by a fixed amount in each breath.

Table 3 presents the results obtained by varying different parameters and their effects on stability. We compile the results for both of the versions of modeling dead space ventilation just described. To develop this table we start with the standard parameter values and the calculated τ^* multiplier for these parameters. Small changes in the constant values for $P_{V_{CO_2}}$ and $P_{V_{O_2}}$ are included as predicted by the five-dimensional model for large parameter changes. Column 1 gives the parameter which is changed while others are held fixed. Column 2 gives the change in that parameter by a certain factor. Column 3 gives the factor by which the standard value for the τ^* multiplier is increased or decreased when this parameter change occurs. Changes in cardiac output are considered below. We see that an increase in lung compartment volumes tends to stabilize the system which agrees with [4]. It is interesting to note that using $V_{\text{eff}} = V \Leftrightarrow V_D$ to represent dead space ventilation acts to reduce the stability of the system more than the factor E_F does. This makes sense if we consider that E_F acts to reduce the effectiveness of the control signal by a certain constant percent while in the expression $V_{\text{eff}} = V \Leftrightarrow V_D$ the useless volume V_D becomes a smaller percentage as deeper breaths are taken and hence increasing the efficacy of the control. In actuality, the control signal modulates both rate and depth of breathing.

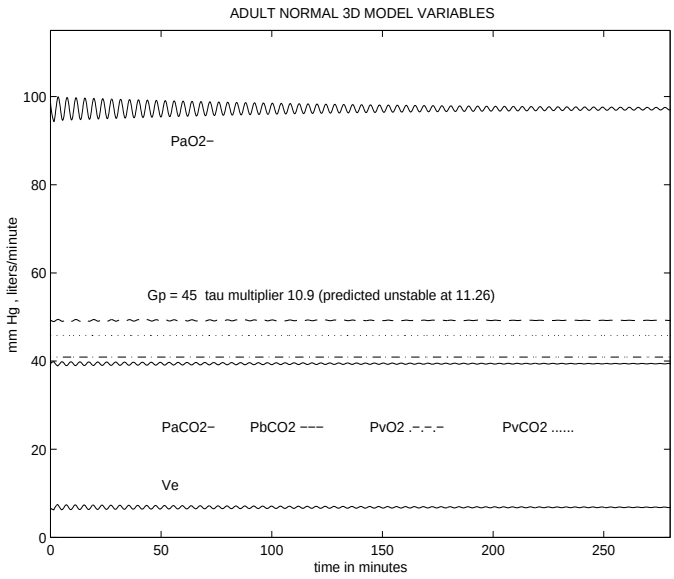

Figure 3: Three-dimensional model stability simulation

The analytical methods described above can predict the effects of any combination of factors as well. From Table 3, one can ascertain the general effects of any combination of factors. We will look at the effect of varying cardiac output in the next section.

2.3 Congestive Heart Condition

Here $\dot{Q}$ is reduced to reflect the inefficient flow of blood. Tables 4 and 5 gives the congestive heart condition calculations for stability. Figures 6 to 8 show simulation results for this case. Figure 6 and Table 4 looks at the case where $\dot{Q}$ is reduced to 4.5 liters/min. Notice that the delay time for instability is much lower than is the case for a normal adult as depicted in Table 3. Figures 7 and 8, and Table 5 reflect the condition where $\dot{Q}$ is reduced to 3.5 liters/minute. Here $P_{a_{CO_2}}$ is increased and $P_{a_{O_2}}$ is reduced as is seen in the clinical setting.

In Figure 7, instability occurs at $\tau^* > 2.8\tau_{\text{norm}}$ where τ_{norm} is now much larger due to the lowered blood flow rate. For higher control gain of 2.5 times normal gain the system is nearly unstable at the normal delay time for this case. Figure 8 reflects the state where the constant V_D replaces E_F in the system. Here the system is driven by the oscillations to apneic periods with cycle time approximately 45 seconds which is in the range of clinical observations (cycle time average 1 minute) [4]. At twice normal gain the system is already unstable at the normal delay time. Table 6 gives the parameter changes for the congestive heart case simulations.

3 Conclusions

Based on the foregoing analysis, we conclude that:

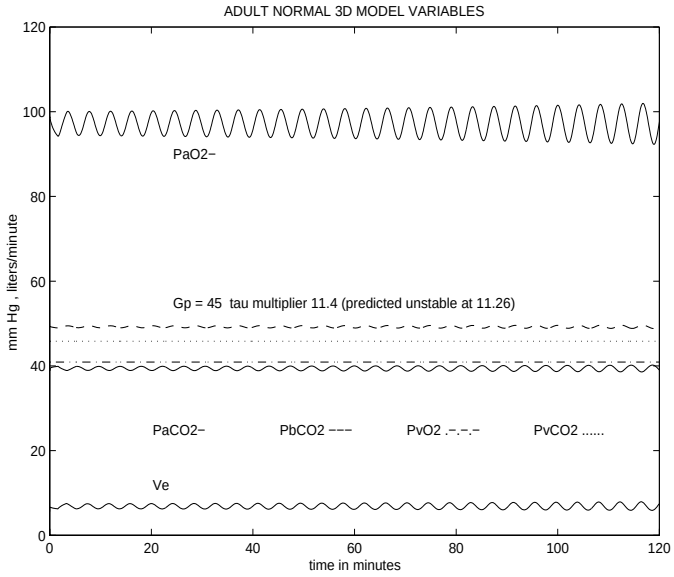

Figure 4: Three-dimensional model unstable simulation

1. The central control acts to reduce the instability inherent in the peripheral control mechanism. One might be tempted to believe that the central control evolved for this purpose. The peripheral control responds quickly to changes in the blood gases while the central control responds more slowly and with less variation due to the process of transforming $P_{a_{CO_2}}$ levels into $P_{B_{CO_2}}$ levels. Peripheral response is most critical during hypoxia and in such cases quick changes in ventilation are necessary. Quick changes to increased $P_{a_{CO_2}}$ and hence decreases in pH levels are also important. The price paid for this response is instability and the central control acts to mitigate this factor.

2. The tissue compartments act to dampen oscillations and contribute to stability as Table 2 indicates. Notice that the five-dimensional model seems to be more stable than the three-dimensional model. Also, Table 3 indicated an increase in lung compartment volumes tends to stabilize the system.

3. Cardiac output increases $P_{V_{CO_2}}$ and $P_{V_{O_2}}$ levels and can create conditions where the delay is small enough for the system to be driven to apneic episodes. This can happen if the controller gain is higher than normal. Note that we did not have to reduce $\dot{Q}$ as drastically as was done in [4] to produce these instabilities.

4. Variations in controller gain are critical to the stability of the system.

5. A control which varies depth of breathing is more unstable than one which varies rate of breathing.

6. Khoo et al [4] analyzed a similar reduced model using Laplace transform and transfer functions. Stability characteristics were represented via Nyquist plots.

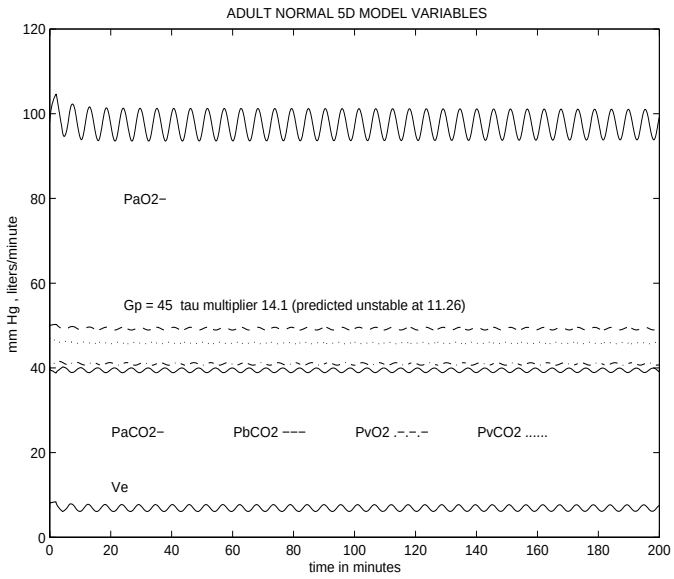

Figure 5: Five-dimensional model unstable simulation

Normal loop gain was given as 0.17 and instability begins when loop gain equals 1. They found that increasing controller gain by 25% increased loop gain by the same amount. Extrapolating from this one would expect that instability would occur when controller gain was increased by about 5.5 times. This correlates with our results that found the delay time for instability was 6.3 times normal delay when a constant dead space was used. We also found that doubling controller gain reduced the delay necessary for instability by not quite one half. Of course, it is important to keep in mind that changing controller gain changes the steady state values and we modified the levels of $P_{V_{CO_2}}$ and $P_{V_{O_2}}$ to reflect this fact. We used the full model to calculate reasonable values for these quantities.

References

[1] Grodins, F.S., Buell, J., and Bart, A.J. Mathematical analysis and digital simulation of the respiratory control system. *J. Appl. Physiology*, 22(2):260–276, 1967.

[2] Hale, J.K. and Verduyn Lunel,S.M. *Introduction to Functional Differential Equations*. Springer-Verlag, N.Y., 1993.

[3] Khoo, M.C.K., Gottschalk, A., and Pack, A.I. Sleep-induced periodic breathing and apnea: A theoretical study. *J. Applied Physiol.*, 70(5):2014–2024, 1991.

[4] Khoo, M.C.K, Kronauer, R.E., Strohl, K.P., and Slutsky, A.S. Factors inducing periodic breathing in humans: a general model. *J. Appl. Physiol.*, 53(3):644–659, 1982.

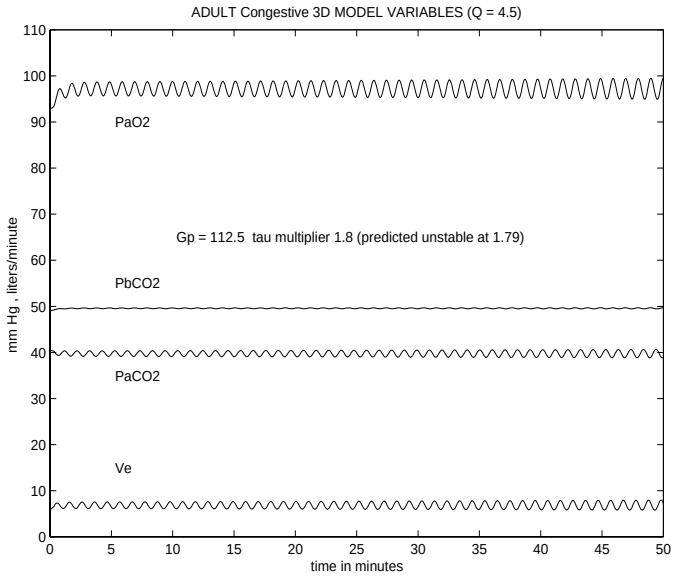

Figure 6: Congestive heart condition: cardiac output 4.5 l/min

Table 1: Stability calculation parameters for Figures 3 and 4

Quantity	Unit	Value
G_C	l/min/mm Hg	1.2
G_P	l/min/mm Hg	45.0
$\dot{Q}$	l/min	6.0
$P_{V_{CO_2}}$	mm Hg	45.8
$P_{V_{O_2}}$	mm Hg	40.9
ω_o	.....	1.51
normal τ	sec	8.5
unstable τ multiplier	...	11.26
$\bar{x}$	mm Hg	39.41
$\bar{y}$	mm Hg	48.74
$\bar{z}$	mm Hg	49.23
$\bar{V}$	l/min	6.83
V_P	l/min	1.54
V_C	l/min	5.29

Table 2: Stability calculation comparisons for 2-D, 3-D,and 5-D models

Quantity	2-D	3-D	5-D
G_C	...	1.2	1.2
G_P	45.0	45.0	45.0
$\dot{Q}$	6.0	6.0	6.0
ω_o	7.82	1.51	...
normal τ	8.5	8.5	8.5
unstable τ multiplier	1.94	11.26	14.1 estimate
$\bar{x}$	41.19	39.41	39.46
$\bar{y}$	64.44	48.75	48.53
$\bar{z}$	...	49.23	49.28
$\bar{V}$	4.70	6.83	6.12
$P_{V_{CO_2}}$	45.8	45.8	45.8
$P_{V_{O_2}}$	40.9	40.9	40.9

Table 3: Stability results of parameter changes for 3-D model

3-D with $\mathbf{E_F} = 0.7$

Quantity	parameter multiplier	τ^* multiplier
G_P and G_C	1.0	11.26 x
G_P and G_C	2.0	5.5 x
$M_{L_{CO_2}}$ and $M_{L_{O_2}}$	0.5	10.99 x
$M_{L_{CO_2}}$ and $M_{L_{O_2}}$	2.0	12.6 x

3-D with $\mathbf{V_D} = 2.0$ l/min

Quantity	parameter multiplier	τ^* multiplier
G_P and G_C	1.0	5.67 x
G_P and G_C	2.0	3.09 x
$M_{L_{CO_2}}$ and $M_{L_{O_2}}$	0.5	4.5 x
$M_{L_{CO_2}}$ and $M_{L_{O_2}}$	2.0	7.05 x

Table 4: Stability calculation parameters for Figure 6

Quantity	Unit	Value
G_P	l/min/mm Hg	45.0
G_C	l/min/mm Hg	1.2
$\dot{Q}$	l/min	4.5
ω_o at normal gain	.....	2.58
ω_o at 2.5 x normal gain	.....	6.14
normal τ	sec	11.3
unstable τ multiple at normal gain	....	4.63
unstable τ multiple at 2.5 x normal gain	....	1.79
$\bar{x}$	mm Hg	39.76
$\bar{y}$	mm Hg	48.79
$\bar{z}$	mm Hg	49.59
$\bar{V}_p$	l/min	1.53
$\bar{V}_c$	l/min	5.29
$P_{V_{CO_2}}$	mm Hg	48.34
$P_{V_{O_2}}$	mm Hg	33.76

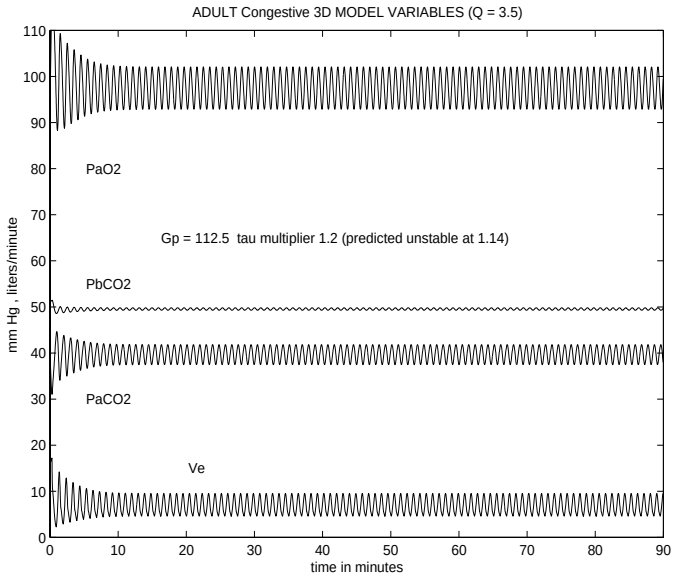

Figure 7: Congestive heart condition: cardiac output 3.5 l/min and high gain

Table 5: Stability calculation parameters for Figures 7 to 8

Figure	Quantity	Unit	Value
Figure 7			
	G_P	l/min/mm Hg	112.0
	G_C	l/min/mm Hg	3.0
	$\dot{Q}$	l/min	3.5
	ω_o at normal gain	.....	3.15
	ω_o at 2.5 x normal gain	.....	7.10
	normal τ	sec	14.6
	unstable τ multiple at normal gain	...	2.82
	unstable τ multiple at 2.5 x normal gain	....	1.14
	$\bar{x}$	mm Hg	39.76
	$\bar{y}$	mm Hg	48.79
	$\bar{z}$	mm Hg	49.58
	$\bar{V}_p$	l/min	1.54
	$\bar{V}_C$	l/min	5.29
	$P_{V_{CO_2}}$	mm Hg	50.79
	$P_{V_{O_2}}$	mm Hg	25.57
Figure 8			
	G_P	l/min/mm Hg	112.5
	G_C	l/min/mm Hg	3.0
	$\dot{Q}$	l/min	3.5
	ω_o at normal gain	.....	4.91
	ω_o at 2.5 x normal gain	.....	10.04
	normal τ	sec	14.6
	unstable τ multiple at normal gain	...	1.76
	unstable τ multiple at 2.0 x normal gain	....	0.77
	$\bar{x}$	mm Hg	39.87
	$\bar{y}$	mm Hg	48.95
	$\bar{z}$	mm Hg	49.70
	$\bar{V}_p$	l/min	1.65
	$\bar{V}_C$	l/min	5.63
	$\dot{V}_D$	l/min	2.00
	$P_{V_{CO_2}}$	mm Hg	50.91
	$P_{V_{O_2}}$	mm Hg	25.56

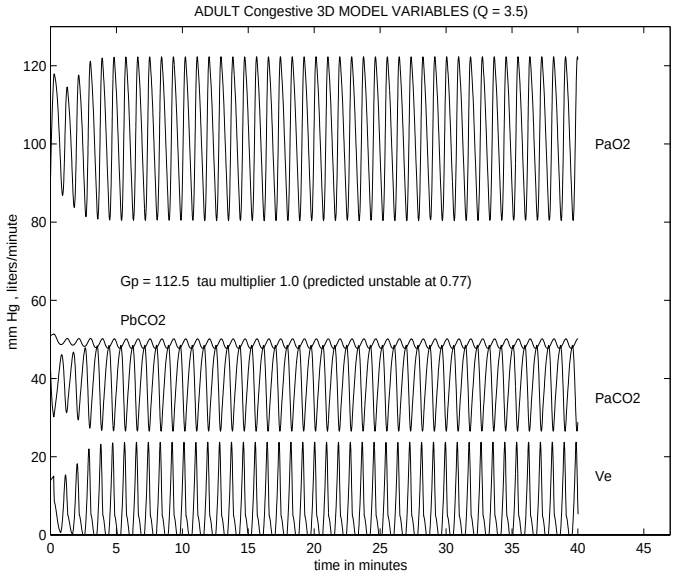

Figure 8: Congestive heart condition: cardiac output 3.5 l/min and high gain

Table 6: Stability calculation model parameter changes for Fig. 6-8

Figure	Quantity	Unit	Value
Figure 6			
	G_P	l/min/mm Hg	45.0
	G_C	l/min/mm Hg	1.2
	$\dot{Q}$	l/min	4.5
	$\bar{x}$ at normal gain	mm Hg	42.03
	$\bar{y}$ at normal gain	mm Hg	51.57
	$\bar{z}$ at normal gain	mm Hg	51.86
	$P_{V_{CO_2}}$ at normal gain	mm Hg	50.60
	$P_{V_{O_2}}$ at normal gain	mm Hg	33.43
	$\bar{V}_P$ at normal gain	l/min	1.61
	$\bar{V}_C$ at normal gain	l/min	4.83
	I_P	mm Hg	38.0
	I_C	mm Hg	38.0
	E_F	...	0.7
Figure 7			
	G_P	l/min/mm Hg	45.0
	$\bar{x}$ at normal gain	mm Hg	42.07
	$\bar{y}$ at normal gain	mm Hg	51.60
	$\bar{z}$ at normal gain	mm Hg	51.85
	$P_{V_{CO_2}}$ at normal gain	mm Hg	53.06
	$P_{V_{O_2}}$ at normal gain	mm Hg	25.25
	$\bar{V}_P$ at normal gain	l/min	1.62
	$\bar{V}_C$ at normal gain	l/min	4.83
	I_P	mm Hg	38.0
	I_C	mm Hg	38.0
	E_F	...	0.7
Figure 8			
	G_P	l/min/mm Hg	45.0
	G_C	l/min/mm Hg	1.2
	$\dot{Q}$	l/min	3.5
	$\bar{x}$ at normal gain	mm Hg	42.34
	$\bar{y}$ at normal gain	mm Hg	51.99
	$\bar{z}$ at normal gain	mm Hg	52.16
	$P_{V_{CO_2}}$ at normal gain	mm Hg	53.37
	$P_{V_{O_2}}$ at normal gain	mm Hg	25.19
	$\bar{V}_P$ at normal gain	l/min	1.77
	$\bar{V}_C$ at normal gain	l/min	5.20
	I_P	mm Hg	38.0
	I_C	mm Hg	38.0
	E_F	...	0.9
	$\dot{V}_D$	l/min	2.0

Table 7: Parameter values for 3-D model

Quantity	Unit	Value
G_C	l/min/mm Hg	1.2
G_P	l/min/mm Hg	45.0
$\dot{Q}$	l/min	6.0
$\dot{Q}_B$	l/min	0.75
$P_{V_{CO_2}}$	mm Hg	45.8
$P_{V_{O_2}}$	mm Hg	40.9
I_P	mm Hg	35.0
I_C	mm Hg	35.0
$M_{L_{CO_2}}$	liter	3.2
$M_{L_{O_2}}$	l/min	2.5
EF	mm Hg	0.7
$P_{I_{O_2}}$	mm Hg	146.0
K_{CO_2}	mm Hg	0.0057
m_a	mm Hg	0.00025
B_a	mm Hg	0.1728
m_v	mm Hg	0.0021
B_v	l/min/mm Hg	0.0662
$MR_{B_{CO_2}}$	mm Hg	0.042
$M_{B_{CO_2}}$	mm Hg	0.9
V_D	l/min	2.0